Cooperative Strategies for Distributed Full-Duplex Relay Networks with Limited Dynamic Range

Omid Taghizadeh and Rudolf Mathar
Institute for Theoretical Information Technology
RWTH Aachen University, D-52074 Aachen, Germany
Email: {taghizadeh, mathar}@ti.rwth-aachen.de

***Abstract*—In this work we study cooperative communication schemes which can benefit from a full-duplex (FD) operation. In particular, we exploit natural characteristics of satellite communication channels which allow for a full-duplex and simultaneous operation of nodes. These characteristics result in significant gains when applied to the well-known cooperative communication schemes. We start our study by defining a system of amplify-and-forward (AF) relay network where relay nodes are empowered with FD capability. We incorporate the limits of FD nodes for suppressing the inherent loopback self-interference. Afterwards we derive optimal relay selection and optimal distributed beamforming, given the global or local channel state information. We show that optimal solutions for the aforementioned problems can be achieved in polynomial time. At the end, we evaluate the effectiveness of the proposed algorithms and the defined system compared to the half-duplex counterpart.**

I. Introduction

Full-duplex (FD) is defined as the capability to transmit and receive at the same time and frequency. Although FD schemes are beneficial in many desired aspects , e.g., lower delay, higher efficiency and security, they were long considered to be practically infeasible due to the inherent self-interference. Recently, specialized cancellation techniques have provided adequate level of isolation between transmit (Tx) and receive (Rx) directions to facilitate a FD communication [1]–[9]. The reported result in [6] promises a suppression of self-interference down to the receiver noise floor throughout the bandwidth of 80 MHz (compliant with IEEE 802.11ac). Hence it becomes more interesting to detect and investigate classic half-duplex (HD) schemes which may benefit from FD operation. As a clear candidate for incorporating the FD operation we can update the satellite-to-satellite communication with this capability. This directly benefits the aforementioned communication schemes with intrinsic advantageous of FD systems such as lower delay, spectral efficiency and security [10]. Full-duplex operation is particularly interesting for satellite nodes as the high directivity of the used antennas, together with multi-path free nature of the self interference channel allow for effective isolation of Tx and Rx directions [11], [12]. The aforementioned characteristic also facilitates simultaneous function of multiple FD satellite nodes which will be better explained in the rest of the paper. Furthermore, it is important to note that although the proposed cancellation techniques increase the cost of the radio front-ends which is a financial challenge for low cost technologies, this is not a big issue for a satellite node.

In this work, we study how FD operation is beneficial for cooperative communication schemes in the light of space and wireless satellite communications. More specifically, we look at a scenario where two end users are communicating with the help of a relay network, where relay nodes are capable of FD operation. At the first glance, the simultaneous reception and transmission in the same channel (FD) may be harmful for some cooperative schemes due to the resulting inter-relay interference (IRI). The aforementioned effect (IRI) limits the gainful use of cooperative FD operation to two cases where i) one FD relay is selected and used to forward the massage and hence the IRI is avoided or (ii) only a set of relay nodes are used which are in deep fade or week channel condition with respect to each other. The second case (ii) is specially interesting for the space and satellite-to-satellite communications where IRI can be avoided due to multipath-free nature of the channel, as well as the highly directive antennas in each node. Studies on applying FD operation on a relay node [3], [13]–[16] and in particular relay selection strategies (where only one FD relay is active) are reported in [17]–[19] where fewer works has been done on the second scenario [20], [21]. Nevertheless none of the previous works apply a realistic model for the behavior of the FD nodes which is essential for a reliable design.

Contribution: Our first contribution is to obtain an optimal FD-relay selection strategy in closed form, for the case where only one relay node is used. A similar scenario has been also studied in [17] for relay selection and performance analysis. Nevertheless they assume a residual self-interference model in FD nodes with constant variance, similar to an additional white noise component. While this approach provides an easy design, this is not realistic since the residual error highly depends on the strength of the loop-back interference signal. We incorporate the more accurate model for FD operation which is proposed by [3], [22] based on the system measurement and analysis [23], [24]. As the next step, we consider the simultaneous function of multiple FD relays and study the distributed beamforming problem to deliver the best end-to-end communication rate. We solve the corresponding problem and provide an efficient polynomial-time solution. A sub-optimal design for the similar scenario is also provided where the design of each relay node is done locally, based on its own channel conditions with no information from other nodes. Hence the channel state information (CSI) is not communicated through the network and the required overhead is reduced.

In this document we provide a detailed system model and signal flow in Section II. An optimal relay selection scheme based on the defined model is then presented in Section III. The optimal function of the network for multiple simultaneously active relay nodes is then investigated in Section IV for the scenarios where local or global CSI is available in all nodes. Finally, the simulative evaluation of our solution shows the effectiveness of the proposed methods in Section V.

Mathematical Notation: Throughout this paper, vectors and matrices are denoted as lower-case and upper-case bold letters, respectively. The rank of a matrix, expectation, trace, conjugate and Hermitian transpose are denoted by $\text{rank}(\cdot)$, $\mathbb{E}(\cdot)$, $\text{tr}(\cdot)$, $(\cdot)^*$ and $(\cdot)^{\text{H}}$, respectively. The identity matrix with dimension n is denoted as $\boldsymbol{I}_n$ and $\text{diag}(\cdot)$ fills all non-diagonal elements of a matrix by zero. The set of all positive semi-definite matrices with Hermitian symmetry is denoted by $\mathcal{H}$.

II. System Model

We investigate a scenario where a pair of single antenna, HD users communicate with the help of a rely network where the direct link between the end nodes is ignored. Each relay node is equipped with single Tx and single Rx antenna which facilitate the FD operation. Relays operate in the amplify-and-forward (AF) mode. The wireless channels are assumed to be accurately known in the corresponding relay node and follow the block flat fading model. We name the channel between the source and relay as $h_{\text{sr},k} \in \mathbb{C}$, the loopback self-interference channel (between the transmit and receive antennas of the same relay) as $h_{\text{rr},k} \in \mathbb{C}$ and the relay to the destination as $h_{\text{rd,k}} \in \mathbb{C}$ where k represents the index of the relay node. The variance of the respective channel coefficients are denoted by $\rho_{\text{sr},k}, \rho_{\text{rd},k}, \rho_{\text{rr}} \in \mathbb{R}^+$. The index set of all available relay nodes in the network is denoted as $\mathbb{F}$ while the index set of all relay nodes which contribute in the communication process (active nodes) is denoted as $\mathbb{K}$. Without loss of generality we assume the indexes of the active relay nodes are assigned such that $\mathbb{K} = \{1, 2, \cdots, |\mathbb{K}|\}$ where $|\mathbb{K}|$ represents the size of the set. In our work, we assume that the active FD relay nodes do not make inter-relay interference on each other. This assumption holds for the scenario with only one active relay (single relay selection), as well as the scenarios of satellite-to-satellite communication where isolation of relay nodes can be achieved due to absence of multi-path propagation, and exploiting highly directive antennas.

A. Source-to-relay communication

Each active relay node continuously receives and amplifies the received signal from the source, while dealing with the loopback interference signal from its own transmitter front-end. This is done by utilizing the known self-interference cancellation techniques [2]–[6] in the receiver front-end. The received signal on the relay is

$$r_{\text{in},k} = \underbrace{h_{\text{sr},k} \cdot s + h_{\text{rr},k} \cdot r_{\text{out},k} + m_k}_{u_{\text{in},k}} + e_{\text{in},k} \quad (1)$$

where $r_{\text{in},k}, r_{\text{out},k} \in \mathbb{C}$ respectively represent the received and transmitted signal at the k-th relay node and $m_k \in \mathbb{C}$ represents the zero-mean circularly symmetric complex Gaussian (ZMCSCG) noise with variance M_k. The transmitted signal from the source is represented as $s \in \mathbb{C}$ and $u_{\text{in},k} \in \mathbb{C}$ is the *undistorted* received signal on the Rx antenna. The receiver distortion, as the additional distortion from antenna up to ADC module is represented as $e_{\text{in},k} \in \mathbb{C}$ which represents the effect of limited dynamic range in facing with the high-power received signal. While the aforementioned distortion is assumed to be ignorable in many classic HD schemes, it plays an important role in FD systems. This stems in the high strength of self-interference (loopback) channel as the distortion signal components remain as the residual interference after self-interference cancellation [3], [22]. The known (distortion-free) part of the self-interference signal is then suppressed and the resulting signal is amplified to constitute the relay's output:

$$r_{\text{out},k} = \underbrace{a_k \cdot r_{\text{supp},k}}_{u_{\text{out},k}} + e_{\text{out},k}, \quad (2)$$

$$r_{\text{supp},k} = r_{\text{in},k} - h_{\text{rr},k} \cdot u_{\text{out},k}, \quad (3)$$

where $r_{\text{supp},k} \in \mathbb{C}$ and $a_k \in \mathbb{C}$ represent the interference-suppressed version of received signal and the amplification coefficient at the k-th relay. The *intended* transmit signal is denoted as $u_{\text{out},k}$. Similar to the defined distortion in the receiver chain, we define the transmitter distortion as $e_{\text{out},k}$ which represents the effect of limited transmitter dynamic range. For detailed elaboration of this distortion model please refer to [3], [22] and system measurements in [23], [24]. As it has been shown, the variance of the distortion components is proportional to the collected power on the receiver antenna (undistorted received signal), for $e_{\text{out},k}$, and to the power of the transmit signal prior to DAC module (intended Tx signal), for $e_{\text{out},k}$:

$$\mathbb{E}\{e_{\text{in},k} e^*_{\text{in},k}\} = \beta_k \cdot \mathbb{E}\{u_{\text{in},k} {u_{\text{in},k}}^*\}, \quad \forall k \in \mathbb{K}, \quad (4)$$

$$\mathbb{E}\{e_{\text{in},k} e^*_{\text{in},l}\} = 0, \quad k \neq l, \quad (5)$$

$$\mathbb{E}\{e_{\text{out},k} e^*_{\text{out},k}\} = \gamma_k \cdot \mathbb{E}\{u_{\text{out},k} {u_{\text{out},k}}^*\}, \quad \forall k \in \mathbb{K}, \quad (6)$$

$$\mathbb{E}\{e_{\text{out},k} e^*_{\text{out},l}\} = 0, \quad k \neq l, \quad (7)$$

where $\beta_k, \gamma_k \in \mathbb{R}^+$ are coefficients respectively relating the received and transmitted power to the variance of the resulting distortion. As we will later elaborate, the aforementioned dependencies change the behaviour of the system and lead to the new problem structure. The transmit power of the relay nodes are limited by the allowed individual power range, as well as the limit on total network power consumption:

$$\mathbb{E}\{r_{\text{out},k} r^*_{\text{out},k}\} \leq P_{\text{max}}, \quad \forall k \in \mathbb{K}, \quad (8)$$

$$\sum_{k \in \mathbb{K}} \mathbb{E}\{r_{\text{out},k} r^*_{\text{out},k}\} \leq P_{\text{tot}}, \quad (9)$$

where $P_{\text{max}}, \ P_{\text{tot}}$ respectively represent the individual and total power constraints on the function of the relay nodes.

B. Relay-to-destination communication

The transmitted signals from the relay nodes, pass through the relay to destination channels and constitute the received signal:

$$y = \sum_{k \in \mathbb{K}} h_{\text{rd},k} r_{\text{out},k} + w, \quad (10)$$

where $y, w \in \mathbb{C}$ respectively represent the received signal at the destination and the ZMCSCG noise with variance W. Table I provides the description of all signal notations to better communicate the defined model. In the following, we study the problems regarding relay selection as well as the achievable gains via optimal distributed beamforming in the defined system.

TABLE I: List of the used symbols in the defined system

Notation	Description
s, P_s	transmit signal from the source and its power;
$h_{\text{sr},k}$	source-relay channel coefficients;
$h_{\text{rd},k}$	relay-destination channel coefficients;
$h_{\text{rr},k}$	self-interference channel coefficients;
γ_k, β_k	ratios representing Tx and Rx chains accuracy ;
a_k	relay amplification coefficient;
m_k, M_k	the additive white noise in the relay and its variance;
w, W	the additive white noise in the destination and its variance;
$e_{\text{in},k}$	error signals originating from Rx chains;
$e_{\text{out},k}$	error signals originating from Tx chains;
$r_{\text{in},k}$	received signals at the relay node;
$r_{\text{out},k}$	transmit signals from the relay node;
$u_{\text{in},k}$	non-distorted received signals;
$u_{\text{out},k}$	non-distorted transmit signals;
$P_{\max}$	maximum individual allowed power for rely nodes;
P_{tot}	maximum total allowed power for rely nodes;
$\mathbb{F}$	index set of all relay nodes in the network;
$\mathbb{K}$	index set of active relay nodes in the network;
y	delivered signal at the destination;

III. Optimal Relay Selection

In this section we derive an optimal relay selection strategy which leads to the maximum end to end communication rate. Due to the single antenna, single stream setup we equivalently define our problem as signal-to-error-plus-noise-Ratio (SENR) maximization on the destination user. Our problem can be hence formulated as

$$\max_{k\in\mathbb{F}} \max_{a_k\in\mathcal{A}_k} \text{SENR}_k, \tag{11}$$

where $\mathcal{A}_k$ includes all values of a_k which satisfy the relay's transmit power constraint. In order to solve the above problem, in the first step, we derive an explicit formulation for the relay's transmit power which plays an important role in the formulation of SENR elements. By incorporating (1), (4)-(7) into (2) and (3) we have

$$\mathbb{E}\{u_{\text{out},k}u^*_{\text{out},k}\} = |a_k|^2 \Big(P_s\,|h_{\text{sr},k}|^2 + M_k + \mathbb{E}\{u_{\text{in},k}u^*_{\text{in},k}\}\cdot\beta_k + \mathbb{E}\{u_{\text{out},k}u^*_{\text{out},k}\}\cdot|h_{\text{rr},k}|^2\,\gamma_k\Big). \tag{12}$$

where $P_s := \mathbb{E}\{ss^*\}$ is the transmit power from the source. At this point we recall that due to the proximity of the Rx and Tx antennas on the FD device, the loopback self-interference signal is much stronger than the desired signal which is coming from a distant location (e.g., up to 100 dB according to [22]). Hence the received power at the relay can be safely approximated by the loopback self-interference power

$$\mathbb{E}\{u_{\text{in},k}u^*_{\text{in},k}\} \approx |h_{\text{rr},k}|^2\,\mathbb{E}\{r_{\text{out},k}r^*_{\text{out},k}\}, \tag{13}$$

which by incorporating (13) into (12) and recalling the identity (2) we have

$$\mathbb{E}\{u_{\text{out},k}u^*_{\text{out},k}\}\Big(1-|a_k|^2\Big(|h_{\text{rr},k}|^2\,(\gamma_k+\beta_k+\beta_k\gamma_k)\Big)\Big) = |a_k|^2\Big(P_s\,|h_{\text{sr},k}|^2+M_k\Big). \tag{14}$$

Note that the above derivations (12-14) hold given that all components of the desired signal (s), noise (m_k) and the distortion signals ($e_{\text{in},k}, e_{\text{out},k}$) are zero mean and mutually independent. By incorporating (2) into (14) we write the transmit power from the relay for an arbitrary amplification coefficient a_k as

$$\mathbb{E}\{r_{\text{out},k}\cdot r^*_{\text{out},k}\} = \frac{(1+\gamma_k)\,|a_k|^2\Big(P_s\,|h_{\text{sr},k}|^2+M_k\Big)}{1-|a_k|^2\Big(|h_{\text{rr},k}|^2\,(\gamma_k+\beta_k+\beta_k\gamma_k)\Big)}. \tag{15}$$

In order to obtain an explicit formulation for SENR_k, as the obtained SENR if relay node k is selected, we distinguish the desired as well as the error plus noise parts of the signal power at the receiver. By exploiting the independence among noise, error and signal components we have

$$P_{\text{desired},k} = P_s\cdot|a_k|^2\,|h_{\text{sr},k}h_{\text{rd},k}|^2 \tag{16}$$

$$P_{\text{destructive},k} = |h_{\text{rd},k}|^2\Big(\mathbb{E}\{r_{\text{out},k}\cdot r^*_{\text{out},k}\} - P_s\,|h_{\text{sr},k}|^2\cdot|a_k|^2\Big)+W, \tag{17}$$

where $P_{\text{desired},k}, P_{\text{destructive},k}$ respectively represent the power of the desired and destructive parts of the signal in the destination. The consequent SENR_k is then formulated in (18) assuming an arbitrary amplification coefficient (a_k). It is worth mentioning that the resulting transmit power from each relay, and the consequent link quality (SENR_k) has the different structure compared to the classic scenario with HD relay nodes. This stems in the fact that in the FD scenario the transmit power affects the intensity of the residual self-interference in the receiver via the loopback path, see (1), (4), (6). As the result, the maximum amplification on the relay (corresponding to using the maximum relay individual power) in not necessarily optimal since increasing $|a_k|^2$ simultaneously increases the resulting $P_{\text{destructive},k}$ in a nonlinear fashion. In order to find the optimal value of a_k and the subsequent SENR_k, in the first step we observe from (18) that the value of SENR_k is invariant to $\angle a_k$. Hence we define $\tilde{a}_k := |a_k|^2$ and study the feasibility conditions for values of $\tilde{a}_k$. By incorporating (8) and (9) into (15) we have:

$$0 \le \mathbb{E}\{r_{\text{out},k}r^*_{\text{out},k}\} \le \bar{P}_{\max}, \tag{20}$$

which consequently results in the following upper and lower bounds for $\tilde{a}_k$

$$0 \le \tilde{a}_k,$$

$$\tilde{a}_k \le \bar{P}_{\max}\cdot\Bigg((1+\gamma_k)\Big(P_s\,|h_{\text{sr},k}|^2+M_k\Big) + \bar{P}_{\max}\,|h_{\text{rr},k}|^2\,(\gamma_k+\beta_k+\beta_k\gamma_k)\Bigg)^{-1} =: \tilde{a}_k^{lim}, \tag{21}$$

where $\bar{P}_{\max} := \min(P_{\text{tot}}, P_{\max})$. Note that the obtained upper bound for $\tilde{a}_k$ happens at the upper bound of the inequality in (20), due to monotonic (increasing) nature of $\mathbb{E}\{r_{\text{out},k}r^*_{\text{out},k}\}$ with respect to $\tilde{a}_k$ in the feasible domain. Now we study the behavior of SENR_k function for different values of $\tilde{a}_k$ to obtain the optimum point. As the first step we observe that both extremes of $\tilde{a}_k \to 0$ and $\tilde{a}_k \to \tilde{a}_k^{\infty}$, $\tilde{a}_k^{\infty} := \frac{1}{|h_{\text{rr},k}|^2(\gamma_k+\beta_k+\beta_k\gamma_k)}$, where the relay's transmit power approaches infinity, result in $\text{SENR}_k = 0$. Furthermore, due to the differentiable, positive and continuous nature of SENR_k between these two values, the maximum value of SENR_k

$$\mathrm{SENR}_k = \frac{P_{\mathrm{desired},k}}{P_{\mathrm{destructive},k}} = \frac{P_s \cdot |a_k|^2 \left|h_{\mathrm{sr},k} h_{\mathrm{rd},k}\right|^2}{\left|h_{\mathrm{rd},k}\right|^2 \left(\frac{(1+\gamma_k)|a_k|^2 \left(P_s |h_{\mathrm{sr},k}|^2 + M_k\right)}{1-|a_k|^2\left(|h_{\mathrm{rr},k}|^2 \alpha_k\right)} - P_s \left|h_{\mathrm{sr},k}\right|^2 \cdot |a_k|^2 \right) + W} \tag{18}$$

$$= -1 + \frac{\tilde{a}_k \left((1+\gamma_k) \left|h_{\mathrm{rd},k}\right|^2 \left(P_s \left|h_{\mathrm{sr},k}\right|^2 + M_k \right) - W \left|h_{\mathrm{rr},k}\right|^2 \alpha_k \right) + W}{\tilde{a}_k^2 \left(\alpha_k P_s \left|h_{\mathrm{sr},k} h_{\mathrm{rr},k} h_{\mathrm{rd},k}\right|^2 \right) + \tilde{a}_k \left(-W \left|h_{\mathrm{rr},k}\right|^2 \alpha_k - P_s \left|h_{\mathrm{sr},k} h_{\mathrm{rd},k}\right|^2 + (1+\gamma_k) \left|h_{\mathrm{rd},k}\right|^2 \left(P_s \left|h_{\mathrm{sr},k}\right|^2 + M_k \right) \right) + W} \tag{19}$$

$$\text{where} \quad \alpha_k := \gamma_k + \beta_k + \beta_k \gamma_k, \quad \tilde{a}_k := |a_k|^2 .$$

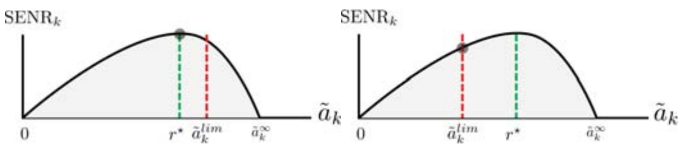

(a) $r^\star \leq \tilde{a}_k^{lim}$ (b) $r^\star > \tilde{a}_k^{lim}$

Fig. 1: Possible situations of $r^\star$ considering the feasible region of $\tilde{a}_k$. The dark circle indicates the position of the optimum point.

occurs at an stationary point (a maximum) between these two values. Note that the SENR_k-maximizing stationary point is not necessarily feasible. By formulating the SENR_k function into the following structure

$$\mathrm{SENR}_k = c_0 + \frac{c_1 \tilde{a}_k + c_2}{d_1 \tilde{a}_k^2 + d_2 \tilde{a}_k + d_3}, \tag{22}$$

where $c_0, c_1, c_2, d_1, d_2, d_3 \in \mathbb{R}$ are directly replaced from (19), we find all stationary points of (19) as

$$\frac{\partial \mathrm{SENR}_k}{\partial \tilde{a}_k} = 0 \quad \Leftrightarrow$$
$$\tilde{a}_k^2 + \tilde{a}_k \left(2\frac{c_2}{c_1} \right) + \left(-\frac{d_3}{d_1} + \frac{d_2 c_2}{d_1 c_1} \right) = 0. \tag{23}$$

The above equality is a classic second order polynomial function with two roots r_1, r_2 as

$$r_1 = -\frac{c_2}{c_1} + \sqrt{\left(\frac{c_2}{c_1}\right)^2 - \frac{c_2 d_2}{c_1 d_1} + \frac{d_3}{d_1}}$$
$$r_2 = -\frac{c_2}{c_1} - \sqrt{\left(\frac{c_2}{c_1}\right)^2 - \frac{c_2 d_2}{c_1 d_1} + \frac{d_3}{d_1}}. \tag{24}$$

It can be proved, that the values of r_1, r_2 are real for the defined system and exactly one of them is a maximum for SENR_k which is located in the range $(0, \tilde{a}_k^{\infty})$. We name this root as $r^\star$ hereinafter. In the following we obtain the optimal value of $\tilde{a}_k$ by observing the characteristics of the SENR function.

As the value of SENR_k is continuous and positive in $\tilde{a}_k \in (0, \tilde{a}_k^{\infty})$, we have $\tilde{a}_k = r^\star$ as the SENR-maximizing point in this region. If $r^\star \leq \tilde{a}_k^{lim}$ (feasibility condition), then $r^\star$ represents the value of optimal $\tilde{a}_k$ (see Fig 1-a). On the other hand, since the SENR_k function has no other extrema in the defined region $(0, \tilde{a}_k^{\infty})$, if $\tilde{a}_k = r^\star$ is located outside of the feasible region (i.e., $r^\star > \tilde{a}_k^{lim}$), then SENR_k is an increasing function of $\tilde{a}_k$ inside its feasible region (see Fig 1-b). In such a case, the optimal $\tilde{a}_k$ is located on the boundary of the feasible region. Hence we always achieve the optimal $\tilde{a}_k$ as

$$\tilde{a}_k^\star = \min\left\{ r^\star, \tilde{a}_k^{lim} \right\}, \quad a_k^\star = \sqrt{\tilde{a}_k^\star}, \tag{25}$$

where $\tilde{a}_k^\star, a_k^\star$ respectively represent the optimal values for $\tilde{a}_k$ and for the relay's amplification coefficient. The obtained optimal link quality (SENR_k) can be consequently achieved via (18). It is worth mentioning that due to the single operation of the selected relay in this scenario, the phase of $a_k^\star$ does not affect the objective as it is clear from (18), (19). Following the same approach for all relays in the network, we achieve the optimal performance of end-to-end communication for the selection of each relay node. Obviously, the relay that offers the highest optimal SENR_k is the one to be selected according to (11).

IV. Distributed Beamforming with Multiple Relay Operation

In this part we extend our scenario to the case where multiple relays are simultaneously active and forward the massage to the destination. Our goal is to obtain the optimal relay amplification coefficients ($a_k, \ \forall k \in \mathbb{K}$) which maximize the end to end link quality. Similar to the previous part we use the signal-to-noise-plus-error ratio as our quality criterion. The respective optimization problem can be hence written as

$$\begin{aligned} \max_{a_k, \forall k \in \mathbb{K}} \quad & \mathrm{SENR}_{\mathbb{K}} \\ \text{s.t.} \quad & \mathbb{E}\{r_{\mathrm{out},k} \cdot r_{\mathrm{out},k}^*\} \leq P_{\max}, \quad \forall k \in \mathbb{K}, \\ & \sum_{k \in \mathbb{K}} \mathbb{E}\{r_{\mathrm{out},k} \cdot r_{\mathrm{out},k}^*\} \leq P_{\mathrm{tot}}. \end{aligned} \tag{26}$$

where $\mathrm{SENR}_{\mathbb{K}}$, represents the achieved SENR with simultaneous operation of all active relays belonging to the set $\mathbb{K}$. It is observable that while the desired signal components which are passing through the relay nodes are highly correlated and represent the same data constellation, the noise and distortion (error) components in the relays and the destination are zero mean and mutually independent. Exploiting the aforementioned property the achieved $\mathrm{SENR}_{\mathbb{K}}$ is formulated in (27) following the similar procedure as (18). Furthermore, the same formulation of the relay transmit power and the feasible regions on $\tilde{a}_k$ for the relay's individual power constraint still holds following (15) and (19). In the following we present an optimization framework to achieve optimal set of $a_k, \forall k \in \mathbb{K}$.

$$\mathrm{SENR}_{\mathbb{K}} = \frac{P_s \left|\sum_{k\in\mathbb{K}} a_k h_{\mathrm{sr},k} h_{\mathrm{rd},k}\right|^2}{W + \sum_{k\in\mathbb{K}} |h_{\mathrm{rd},k}|^2 \left(\frac{(1+\gamma_k)|a_k|^2 \left(P_s |h_{\mathrm{sr},k}|^2 + M_k\right)}{1-|a_k|^2\left(|h_{\mathrm{rr},k}|^2 \alpha_k\right)} - P_s |h_{\mathrm{sr},k}|^2 \cdot |a_k|^2 \right)} \tag{27}$$

$$= \frac{P_s \left|\sum_{k\in\mathbb{K}} a_k h_{\mathrm{sr},k} h_{\mathrm{rd},k}\right|^2}{W + \sum_{k\in\mathbb{K}} \frac{(1+\gamma_k)\left(P_s |h_{\mathrm{sr},k}|^2 + M_k\right)|h_{\mathrm{rd},k}|^2}{\alpha_k |h_{\mathrm{rr},k}|^2} \left(-1 + \frac{1}{1-|a_k|^2 |h_{\mathrm{rr},k}|^2 \alpha_k}\right) - P_s |h_{\mathrm{rd},k} h_{\mathrm{sr},k}|^2 |a_k|^2} \tag{28}$$

A. Optimal Beamforming with maximum link quality

In the first step, we reformulate our objective function with the help of classic matrix operations. This can be done by recalling the $\mathbb{K} := \{1, 2, \cdots, |\mathbb{K}|\}$ as the index set of all relay nodes which contribute in the communication process, and defining the auxiliary vectors $\boldsymbol{b}, \boldsymbol{a} \in \mathbb{C}^{|\mathbb{K}|}$ and diagonal matrices $\boldsymbol{B}_1, \boldsymbol{B}_2, \boldsymbol{B}_3, \boldsymbol{P}_{\mathrm{lim}} \in \mathbb{C}^{|\mathbb{K}|\times|\mathbb{K}|}$ as

$$\begin{aligned}
\boldsymbol{a}[k] &= a_k, \ \forall k \in \mathbb{K}, \\
\boldsymbol{b}[k] &= h_{\mathrm{sr},k} h_{\mathrm{rd},k}, \ \forall k \in \mathbb{K}, \\
\boldsymbol{B}_1[k,l] &= \begin{cases} \frac{(1+\gamma_k)\left(P_s |h_{\mathrm{sr},k}|^2 + M_k\right)|h_{\mathrm{rd},k}|^2}{\alpha_k |h_{\mathrm{rr},k}|^2} & k = l \\ 0 & k \neq l \end{cases} \ \forall k,l \in \mathbb{K}, \\
\boldsymbol{B}_2[k,l] &= \begin{cases} |h_{\mathrm{rr},k}|^2 \alpha_k & k = l \\ 0 & k \neq l \end{cases} \ \forall k,l \in \mathbb{K}, \\
\boldsymbol{B}_3[k,l] &= \begin{cases} |h_{\mathrm{sr},k} h_{\mathrm{rd},k}|^2 & k = l \\ 0 & k \neq l \end{cases} \ \forall k,l \in \mathbb{K}, \\
\boldsymbol{P}_{\mathrm{lim}}[k,l] &= \begin{cases} \tilde{a}_k^{\mathrm{lim}} & k = l \\ 0 & k \neq l \end{cases} \ \forall k,l \in \mathbb{K},
\end{aligned} \tag{29}$$

where for a matrix $\boldsymbol{B}$, $\boldsymbol{B}[k,l]$ represents the element on the k-th row and the l-the column. By incorporating (29) we reformulate (26) as

$$\begin{aligned}
\max_{\boldsymbol{a},t} \ & t \\
\text{s.t.} \ & \frac{P_s \boldsymbol{b}^{\mathrm{T}} \boldsymbol{a}\boldsymbol{a}^{\mathrm{H}} \boldsymbol{b}^*}{\mathrm{tr}\left\{ \boldsymbol{B}_1 \left(-\boldsymbol{I}_{|\mathbb{K}|} + \left(\boldsymbol{I}_{|\mathbb{K}|} - \boldsymbol{B}_2 \mathrm{diag}\left(\boldsymbol{a}\boldsymbol{a}^{\mathrm{H}}\right)\right)^{-1} \right) - P_s \boldsymbol{B}_3 \mathrm{diag}\left(\boldsymbol{a}\boldsymbol{a}^{\mathrm{H}}\right) \right\} + W} \geq t, \\
& \mathrm{tr}\left\{ \boldsymbol{B}_1 \left(-\boldsymbol{I}_{|\mathbb{K}|} + \left(\boldsymbol{I}_{|\mathbb{K}|} - \boldsymbol{B}_2 \mathrm{diag}\left(\boldsymbol{a}\boldsymbol{a}^{\mathrm{H}}\right)\right)^{-1} \right) \right\} \leq P_{\mathrm{tot}}, \\
& \mathrm{diag}\left(\boldsymbol{a}\boldsymbol{a}^{\mathrm{H}}\right) \leq \boldsymbol{P}_{\mathrm{lim}},
\end{aligned} \tag{30}$$

where $\mathrm{diag}(\cdot)$ operator creates a diagonal matrix using the diagonal elements of a matrix, and $t \in \mathbb{R}$ is an auxiliary variable which represents the achievable SENR at the destination. It is observable that if a value of t is achievable for a given system parameters and power constraint (20), then every smaller values of t will be also feasible to achieve. On the other hand if t is not achievable, every bigger value of t will be infeasible as well. Hence, in order to further simplify (30) we apply bi-section search on the values of t to reduce the dimension of the optimization problem. Moreover we define $\boldsymbol{A} := \boldsymbol{a}\boldsymbol{a}^{\mathrm{H}}$ and $\tilde{\boldsymbol{A}} := \mathrm{diag}\left(\boldsymbol{a}\boldsymbol{a}^{\mathrm{H}}\right)$ where $\mathrm{rank}(\boldsymbol{A}) = 1$. By temporary relaxing the inherent rank-1 constraint on $\boldsymbol{A}$ we reformulate (30) as a feasibility check in each step of the bi-section search as

$$\begin{aligned}
\text{find} \ & \tilde{\boldsymbol{A}}, \boldsymbol{A} \\
\text{s.t.} \ & \mathrm{tr}\left\{ -P_s \boldsymbol{b}^* \boldsymbol{b}^{\mathrm{T}} \boldsymbol{A} + t \cdot \boldsymbol{B}_1 \left(-\boldsymbol{I}_{|\mathbb{K}|} + \left(\boldsymbol{I}_{|\mathbb{K}|} - \boldsymbol{B}_2 \tilde{\boldsymbol{A}}\right)^{-1} \right) - t \cdot P_s \boldsymbol{B}_3 \tilde{\boldsymbol{A}} \right\} + t \cdot W \leq 0, \\
& \mathrm{tr}\left\{ \boldsymbol{B}_1 \left(-\boldsymbol{I}_{|\mathbb{K}|} + \left(\boldsymbol{I}_{|\mathbb{K}|} - \boldsymbol{B}_2 \tilde{\boldsymbol{A}}\right)^{-1} \right) \right\} \leq P_{\mathrm{tot}}, \\
& \tilde{\boldsymbol{A}} \leq \boldsymbol{P}_{\mathrm{lim}}, \ \tilde{\boldsymbol{A}} = \mathrm{diag}(\boldsymbol{A}), \\
& \boldsymbol{A}, \tilde{\boldsymbol{A}} \in \mathcal{H},
\end{aligned} \tag{31}$$

where the matrix $\tilde{\boldsymbol{A}}$ is introduced as an auxiliary variable to simplify our notation. It can be proved that the function

$$f(\tilde{\boldsymbol{A}}) = \mathrm{tr}\left\{ \boldsymbol{B}_1 \left(-\boldsymbol{I}_{|\mathbb{K}|} + \left(\boldsymbol{I}_{|\mathbb{K}|} - \boldsymbol{B}_2 \tilde{\boldsymbol{A}}\right)^{-1} \right) \right\}, \tag{32}$$

where $f : \mathcal{D}_{|\mathbb{K}|} \to \mathbb{R}$, is convex over $\tilde{\boldsymbol{A}}$. This is an important observation since as the result, (31) turns into a convex feasibility check and hence can be handled with certainty in polynomial time [25]. Nevertheless, the resulting $\boldsymbol{A}$ is not necessarily a rank-1 matrix which introduces a gap between (30) and the relaxed optimization process. Popular rank-1 approximation and randomization techniques [26] have been developed to handle the similar rank-constraint optimization problems. Luckily, we can always achieve a rank-1 solution for each feasible point of (31). The detailed procedure is not included in this document as it is rather lengthy. By applying the obtained rank-1 solution ($\boldsymbol{A}^\star$), we achieve the set of relay amplification coefficients as

$$\boldsymbol{a}^\star = (\boldsymbol{A}^\star)^{\frac{1}{2}}. \tag{33}$$

The iterations of the defined bi-section search should be continued over t to achieve a desired solution accuracy.

B. System design using local data

In this part, we investigate the case where the design of each amplification coefficient, is done locally on the respective relay node. The channel coefficients ($h_{\mathrm{sr},k}, h_{\mathrm{rd},k}, h_{\mathrm{rr},k}$) and the self-interference cancellation parameters (β_k, γ_k) are assumed to be known in the respective relay node. While this design does not achieve the same performance as the optimal design in the previous part, it is simpler and more robust against the failures of the network data exchange. Nevertheless, the nodes

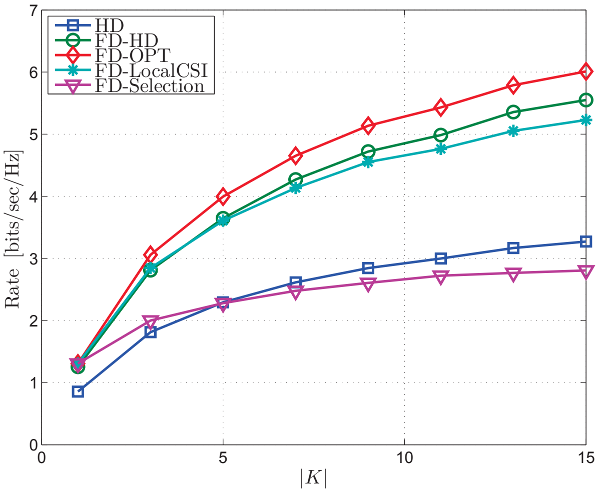

Fig. 2: Rate (bit/sec/Hz) vs. $|\mathbb{K}|$

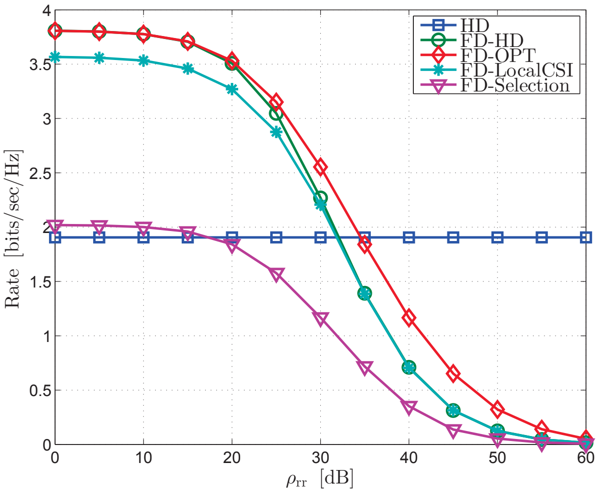

Fig. 3: Rate (bit/sec/Hz) vs. $\rho_{\rm rr}$ (dB)

need to keep the accurate synchronization among each other. According to (27), and the results of triangular inequality, the phase of each amplification coefficient can be optimally adjusted in the respective relay node as

$$\angle \boldsymbol{a}^{\star}[k] = -\angle h_{{\rm sr},k} h_{{\rm rd},k}. \tag{34}$$

The above adjustment of phase elements is feasible assuming the perfect synchronization among the relay nodes. As the result, our problem simplifies to the design of the magnitude of each amplification coefficient in order to maximize the SENR caused by the corresponding node. It can be written as

$$\max_{\tilde{a}_k} {\rm SENR}_k \;\; {\rm s.t.}\; \mathbb{E}\{r_{{\rm out},k} r_{{\rm out},k}^{*}\} \leq \min\left\{\frac{P_{\rm tot}}{|\mathbb{K}|}, P_{\max}\right\}, \tag{35}$$

where the transmit power of the relay is additionally bounded by $\frac{P_{\rm tot}}{|\mathbb{K}|}$ in order to satisfy the total power constraint of the network. The above problem has the similar formulation as in (11) and hence, can be solved following the same procedure.

V. Simulation Results

In this section we evaluate the performance of the introduced methods via Monte Carlo simulations with 500 channel

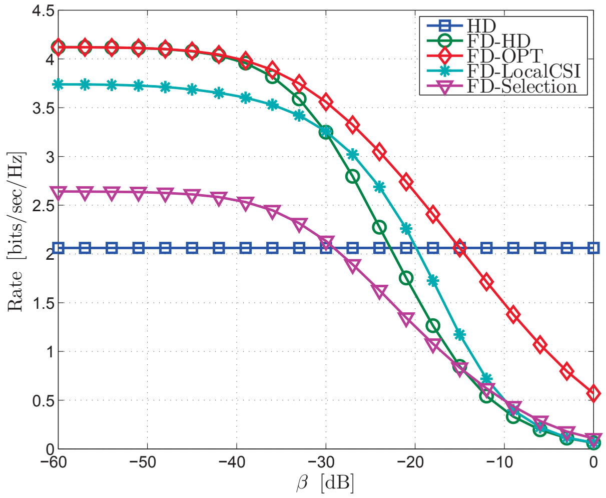

Fig. 4: Rate (bit/sec/Hz) vs. β (dB)

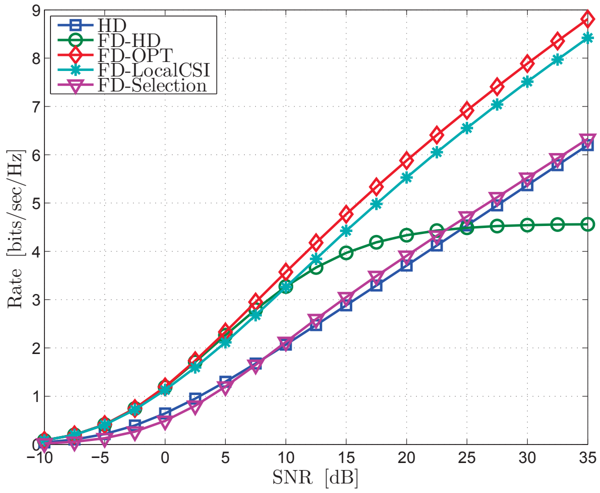

Fig. 5: Rate (bit/sec/Hz) vs. SNR (dB)

realizations. We investigate the effect of the different system parameters and transmit strategies on the resulting performance. The effect of the noise power (SNR $:= \frac{P_{\max}=P_{\rm tot}}{M_k=W}$), hardware distortions and imperfections ($\beta := \beta_k = \gamma_k$), the variance of the loopback channel coefficients ($\rho_{\rm rr}$), and the number of active relay nodes ($|\mathbb{K}|$) are illustrated in Fig. 2 - Fig. 5. In our graphs, 'HD' represents the performance result of the equivalent HD setup (with optimal beamforming), 'FD-HD' represents the performance of the classic HD beamforming applied to our FD setup, 'FD-OPT' represents the optimal FD beamforming solution, 'FD-LocalCSI' corresponds to the solution using the local data for each node, and 'FD-Selection' corresponds to optimal single FD relay selection scheme. Unless stated otherwise, we use the following parameters in our simulations: $\rho_{\rm sr} = 0$dB, $\rho_{\rm rd} = 0$dB, $\rho_{\rm rr} = 20$dB, SNR $= 10$dB, $\beta = -30$dB, $P_{\max} = P_{\rm tot} = 1$, $W = M_k = 1$, $|\mathbb{K}| = 4$. As we have expected, the significant gain of FD system over equivalent HD counterpart is achievable for high system dynamic range (small β) or with proper isolation of Tx and Rx chains (small $\rho_{\rm rr}$). Furthermore, the performance of the classic HD beamforming suffers as the self-interference cancellation quality decreases. Overall, as it is observable from the simulations, the significant gain can be achieved via i) including the self-interference cancellation into the communicating nodes, and enable the FD operation, and ii) by benefiting from simultaneous operation of the FD relay nodes and applying the derived optimal design. It is clear, that the achieved gains are only valid for the communication scenarios where the inter-relay interference (which is inherent to simultaneous operation of FD nodes) could be suppressed. A good example is the scenario of satellite-to-satellite communication where this can be realized due to multipath-free nature of the channels as well as the highly directive antennas on the relay nodes.

VI. Conclusion

In this work we have addressed the design methodology and achievable gains for a cooperative communication scheme which benefits from full-duplex operation at the relay nodes. In particular, we observed the significant gain which is achievable in such a system once the inter-relay and loopback self-interference can be overcame at the relay nodes. Examples of such systems are scenarios of satellite-to-satellite communication, where isolation of relay nodes can be achieved due to absence of multi-path propagation, and exploiting highly directive antennas. The simulations show the significant gains of FD operation on such systems, exploiting the recently-introduced self-interference cancellation techniques together with the proposed optimal designs in the previous sections.

VII. Acknowledgment

Authors would like to thank Dipl.-Ing. Johannes Schmitz, Institute for Theoretical Information Technology, RWTH Aachen University for his fruitful discussions during this work.

References

[1] M. Duarte and A. Sabharwal, “Full-duplex wireless communications using off-the-shelf radios: Feasibility and first results,” in *Proceedings of 44th Asilomar Conference on Signals, Systems, and Computers*, Pacific Grove, CA, Nov. 2010.

[2] J. I. Choi, M. Jain, K. S. P. Levis, and S. Katti, “Achieving single channel, full duplex wireless communication,” in *Proc. 16th Annual Int. Conf. Mobile Computing and Networking (Mobicom 2010)*, Chicago, IL, Sep. 2010.

[3] B. Day, A. Margetts, D. Bliss, and P. Schniter, “Full-duplex MIMO relaying: Achievable rates under limited dynamic range,” *IEEE Journal on Selected Areas in Communications*, vol. 30, pp. 1541–1553, Sep. 2012.

[4] M. Jain, J. I. Choi, T. Kim, D. Bharadia, K. Srinivasan, S. Seth, P. Levis, S. Katti, and P. Sinha, “Practical, real-time, full duplex wireless,” in *Proceedings of 17th Annual International Conference on Mobile Computing and Networking (MobiCom)*, Las Vegas, NV, Sep. 2011.

[5] Y. Hua, P. Liang, Y. Ma, A. Cirik, and G. Qian, “A method for broadband full-duplex MIMO radio,” *IEEE Signal Processing Letters*, vol. 19, Dec. 2011.

[6] D. Bharadia, E. McMilin, and S. Katti, “Full duplex radios,” in *Proceedings of the ACM SIGCOMM*, 2013, pp. 375–386.

[7] R. Askar, T. Kaiser, B. Schubert, T. Haustein, and W. Keusgen, “Active self-interference cancellation mechanism for full-duplex wireless transceivers,” in *Cognitive Radio Oriented Wireless Networks and Communications (CROWNCOM), 2014 9th International Conference on*, June 2014.

[8] A. K. Khandani, “Methods for spatial multiplexing of wireless two-way channels,” Oct. 19 2010, uS Patent 7,817,641.

[9] ——, “Two-way (true full-duplex) wireless,” in *Information Theory (CWIT), 2013 13th Canadian Workshop on*. IEEE, 2013, pp. 33–38.

[10] J. I. Choi, S. Hong, M. Jain, S. Katti, P. Levis, and J. Mehlman, “Beyond full duplex wireless,” in *Signals, Systems and Computers (ASILOMAR), 2012 Conference Record of the Forty Sixth Asilomar Conference on*, Nov 2012, pp. 40–44.

[11] A. S. E. Everett, A. Sahai, “Passive self-interference suppression for full-duplex infrastructure nodes,” *IEEE Transactions on Wireless Communication*, Feb. 2014.

[12] E. Everett, M. Duarte, C. Dick, and A. Sabharwal, “Empowering full-duplex wireless communication by exploiting directional diversity,” in *Proceedings of 44th Asilomar Conference on Signals, Systems, and Computers (Asilomar)*, Pacific Grove, CA, Nov. 2011.

[13] J. Zhang, O. Taghizadeh, and M. Haardt, “Joint source and relay precoding design for one-way full-duplex MIMO relaying systems,” *Proceedings of the Tenth International Symposium on Wireless Communication Systems (ISWCS)*, Aug. 2013.

[14] T. Riihonen, S. Werner, and R. Wichman, “Mitigation of loopback self-interference in full-duplex MIMO relays,” *IEEE Transactions on Signal Processing*, vol. 59, 2011.

[15] O. Taghizadeh and R. Mathar, “Robust multi-user decode-and-forward relaying with full-duplex operation,” in *The Eleventh International Symposium on Wireless Communication Systems (ISWYS 2014)*, Barcelona, Spain, Sep. 2014.

[16] ——, “Full-duplex decode-and-forward relaying with limited self-interference cancellation,” in *Proceedings of International ITG Workshop on Smart Antennas (WSA), Erlangen, Germany*, March 2014.

[17] P. S. I. Krikidis, H. A. Suraweera and C.Yuen, “Full-duplex relay selection for amplify-and-forward cooperative networks,” *IEEE Transactions on Wireless Communications, Vol. 11, No.12*, Dec. 2012.

[18] K. L. Q. Li and K. C. Teh, “Achieving optimal diversity-multiplexing tradeoff for full-duplex MIMO multihop relay networks,” *IEEE Transactions on Information Theory, Vol. 57, No. 1*, Jan. 2011.

[19] I. Krikidis and H. A. Suraweera, “Full-duplex cooperative diversity with alamouti space-time code,” *IEEE Wireless Communication Letters*, 2013.

[20] A. del Coso Sánchez, “Achievable rates for gaussian channels with multiple relays,” Ph.D. dissertation, PhD thesis, Universitat Politecnica de Catalunya, 2008.(Cité en pages 58, 59 et 113.), 2008.

[21] S. D. H. Jiang, X. Xing, “Distributed optimal cyclotomic space-time coding for full-duplex cooperative relay networks,” *9th International Wireless Communications and Mobile Computing Conference (IWCMC)*, 2013.

[22] B. Day, A. Margetts, D. Bliss, and P. Schniter, “Full-duplex bidirectional MIMO: Achievable rates under limited dynamic range,” *IEEE Transactions on Signal Processing*, Jul. 2012.

[23] H. Suzuki, T. V. A. Tran, I. B. Collings, G. Daniels, and M. Hedley, “Transmitter noise effect on the performance of a MIMO-OFDM hardware implementation achieving improved coverage,” *IEEE J. Sel. Areas in Communication*, vol. 26, pp. 867–876, Aug. 2008.

[24] W. Namgoong, “Modeling and analysis of nonlinearities and mismatches in AC-coupled direct-conversion receiver,” *IEEE Trans. Wireless Commun.*, vol. 47, pp. 163–173, Jan. 2005.

[25] S. P. Boyd and L. Vandenberghe, *Convex optimization*. Cambridge University Press, 2004.

[26] Y. Nesterov, “Semidefinite relaxation and nonconvex quadratic optimization,” *Optimization methods and software*, vol. 9, 1998.